AIP | Applied Physics Letters

A unified analytical model of the junction electrostatics in nanowire and nanotube arrays

Vijaya Kumar Gurugubelli and Shreepad Karmalkar

Citation: Applied Physics Letters **104**, 203502 (2014); doi: 10.1063/1.4879261
View online: http://dx.doi.org/10.1063/1.4879261
View Table of Contents: http://scitation.aip.org/content/aip/journal/apl/104/20?ver=pdfcov
Published by the AIP Publishing

A unified analytical model of the junction electrostatics in nanowire and nanotube arrays

Vijaya Kumar Gurugubelli[a] and Shreepad Karmalkar
Department of Electrical Engineering, Indian Institute of Technology Madras, Chennai 600036, India

(Received 10 December 2013; accepted 6 May 2014; published online 21 May 2014)

We establish the unity underlying the junction electrostatics of nanowire and nanotube arrays, and develop a simple analytical model for both based on a common set of approximations of the field/potential distributions. The model predicts large depletion widths accurately, and reveals that, the depletion width in an array of nanowire and nanotube junctions varies as $1/\sqrt{\text{charge per unit length of wire/tube}}$ multiplied by inter-wire/tube separation, where charge per unit length includes the effects of wire/tube radius and doping. This is much different from the exponential form derived in literature for a single nanowire or nanotube junction. The model satisfies all the limiting conditions, matches with numerical simulations and is extendible to nanofilms. Hence, it should be quite useful for nanodevice design. © *2014 AIP Publishing LLC*. [http://dx.doi.org/10.1063/1.4879261]

Early 20th century saw intense efforts to realize vacuum tube devices in semiconductors. Today, similar efforts are on to fabricate conventional diodes and transistors in semiconductor nanowires (NWs)[1] and nanotubes (NTs)[2] to harness the unique properties of materials in the nano-scale. Junction electrostatics governs the behaviour of these NW/NT devices, and can be understood considering NW-metal and NT-metal junctions. Léonard and Tersoff[3] showed that the space-charge width in a NT *p-n* junction is unusually longer than that in the planar bulk junction. Analysis of NW-metal junction[4–6] also revealed similar behavior. Specifically, it was shown that the dependence of the depletion width on doping, radius, and potential drop in the NW/NT is exponential, as against the square root dependence in a planar bulk junction. These analyses are for a single NW/NT[3,5,6] or for a NW in an array with very large inter-wire separation.[4] However, in realistic array geometries, the inter-wire/tube separation is small, and we anticipate that the junction depletion width would be much larger than that of a planar bulk junction but may not follow the exponential dependence of a single NW/NT junction due to mutual screening from surrounding NWs/NTs. Some works[7–9] have studied the physics of these junctions numerically.

We derive a simple, accurate, and unified analytical model of the electrostatics of arrays of NW/NT -metal junctions, extendible to nanofilms. The model is developed based on two new insights regarding the field/potential distribution. First, there is a unity underlying the electrostatics of NW and NT: the field/potential distribution in a NT is analogous to that in a NW array with zero volume-charge but non-zero interface charge and wire dielectric constant equal to ambient dielectric constant. Second, the following approximations of the field/potential distribution in the NW/NT lead to an accurate model matching with numerical simulations: over the wire/tube diameter, the axial field component and the potential are uniform, and the radial field component varies linearly from zero at the axis of symmetry. These approximations apply to a nanofilm as well, and allow a simple analytical solution of the Poisson's equation in the NW/NT and Laplace's equation in the ambient. The resulting model predicts that the depletion width in the NW/NT varies as $1/\sqrt{\text{charge per unit length}}$ multiplied by inter-wire/tube separation, where charge per unit length includes the effects of wire/tube radius and doping. Our model is compared with existing models, and validated with limiting cases and self-consistent numerical calculations. We first present the model for a NW and then replicate it for the NT.

Unlike in a bulk junction, the surrounding field plays a significant role in a NW junction (see Fig. 1).[10] Hence, the junction electrostatics in a NW depends on (see Fig. 2) the radius R and length L of the NW, interwire separation in an array and ambient permittivity ϵ_a, in addition to the potential drop V_d and doping N_A in the NW, and the semiconductor permittivity ϵ_s, which affect a bulk junction. Without loss of generality, we assume that the NW is *p*–type and space-charge is due to depletion of holes.

The potential distribution φ is governed by Poisson's equation in the semiconductor, Laplace's equation in the ambient, and the boundary conditions shown in Fig. 2(b). The condition of zero radial field at $r = S$ is an approximation[11] for a periodic array of wires, where the normal field is zero at the boundary of the Wigner-Seitz unit cell, and S is the radius of an effective cylindrical cell of the same volume as the Wigner-Seitz unit cell. The condition of zero radial field at $r = 0$ follows from cylindrical symmetry. The boundary condition away from the metal plane will be explained shortly.

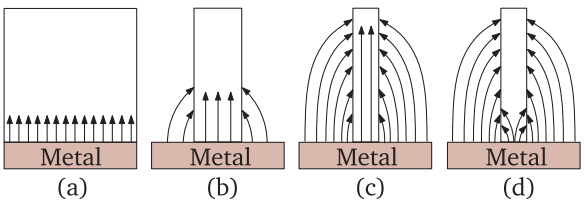

FIG. 1. Internal and surrounding ambient field pictures in a junction between a metal and, a bulk semiconductor (a), a thick NW (b), a thin NW (c), and a NT (d).

[a]Electronic mail: kumar17v@gmail.com

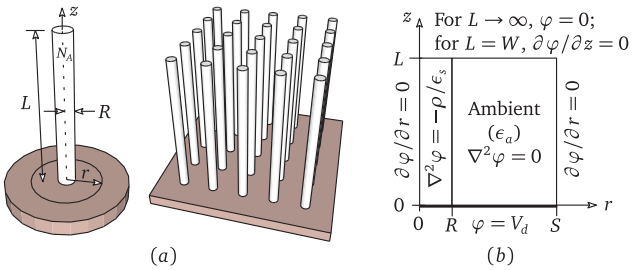

FIG. 2. (a) A NW/NT of radius R and length L, and an array of such NWs/NTs. (b) Right half cross-section of a NW/NT showing the equations and boundary conditions; for a NT, $\rho = 0$, $\epsilon_s = \epsilon_a$, and there is an interface charge at $r = R$.

Our solution is based on three approximations. First, the radial field component E_r, which is zero at $r = 0$, varies linearly to a non-zero value at $r = R$, because R is comparable to or less than the Debye length. Next, φ and the axial field component E_z are uniform over the diameter, because the potential drop over the thickness of a NW is negligible. Since φ versus r is uniform, we are left with solving for φ versus z, taking into account the effect of surrounding field. We obtain a 1D differential equation for φ versus z using the above approximations in the 3D/2D Poisson's equation in the wire, and solve this equation for φ using the general solution of the Laplace's equation in the ambient.

The Poisson's equation inside the NW is

$$\frac{\partial E_r}{\partial r} + \frac{E_r}{r} + \frac{\partial E_z}{\partial z} = \frac{\rho}{\epsilon_s}, \tag{1}$$

where we approximate E_r to increase linearly with r from $E_r = 0$ at $r = 0$, so that

$$\frac{\partial E_r(r,z)}{\partial r} \approx \frac{E_r}{r} \approx \frac{E_r(R^-,z)}{R} = -\frac{1}{R}\frac{\epsilon_a}{\epsilon_s}\frac{\partial\varphi(R^+,z)}{\partial r} \tag{2}$$

and E_z to be constant with r for $r \le R$, i.e.,

$$\frac{\partial E_z(r,z)}{\partial z} \approx \frac{\partial E_z(R^-,z)}{\partial z} = -\frac{\partial^2\varphi(R^+,z)}{\partial z^2}. \tag{3}$$

Note that Eq. (2) assumes zero interface charge. However, including this charge is easy, as will be evident later in the derivation for the NT. We now consider the cases of small and large voltage drop, V_d, in turn. When V_d is small, depletion is partial and linear screening prevails, i.e., the potential and the space-charge inside the semiconductor are linearly related; this analysis gives insight into the unique size effects of nanodevice characteristics, e.g., nano-scale screening influences the field enhancement factor of a NW field emission device.[12] When V_d is large, depletion can be complete and non-linear screening prevails; this analysis is useful for NW schottky diodes.[6]

For linear screening, the space charge density is proportional to the potential as per $\rho = -qN_A\varphi/V_t$, where V_t is the thermal voltage. Further, negligible potential variation over the wire diameter implies $\varphi(r,z) \approx \varphi(0,z) \approx \varphi(R,z)$. Substitution of these results into Eq. (1) leads to the 1D differential equation

$$\frac{2}{R}\frac{\epsilon_a}{\epsilon_s}\frac{\partial\varphi(R^+,z)}{\partial r} + \frac{\partial^2\varphi(R^+,z)}{\partial z^2} = \frac{\varphi(R^+,z)}{L_D^2}, \tag{4}$$

where $L_D = \sqrt{\epsilon_s V_t/qN_A}$ is the Debye length.

For infinitely long wires, $\varphi \to 0$ as $z \to \infty$ and the general solution of the Laplace's equation in the ambient can be written as

$$\varphi(r > R, z) = V_d - \int_0^\infty A(\lambda)\sin(\lambda z) \times \left\{\frac{I_1(\lambda S)K_0(\lambda r) + I_0(\lambda r)K_1(\lambda S)}{I_1(\lambda S)K_0(\lambda R) + I_0(\lambda R)K_1(\lambda S)}\right\} d\lambda, \tag{5}$$

where I_0, I_1 and K_0, K_1 are modified Bessel functions. Using Eqs. (4) and (5), and Fourier Sine Transform, we get

$$A(\lambda) = \frac{2V}{\pi\lambda}\left[1 + 2\frac{\epsilon_a}{\epsilon_s}\frac{L_D^2}{R}\lambda T(\lambda) + L_D^2\lambda^2\right]^{-1}, \tag{6}$$

where

$$T(\lambda) = \frac{I_1(\lambda S)K_1(\lambda R) - I_1(\lambda R)K_1(\lambda S)}{I_1(\lambda S)K_0(\lambda R) + I_0(\lambda R)K_1(\lambda S)}. \tag{7}$$

Combining Eqs. (5)–(7), we get φ as a function of z as

$$\frac{\varphi(R^+,z)}{V_d} = 1 - \frac{2}{\pi}\int_0^\infty \frac{\sin(\lambda z)/\lambda}{1 + 2\frac{\epsilon_a}{\epsilon_s}\frac{L_D^2}{R}\lambda T(\lambda) + L_D^2\lambda^2} d\lambda. \tag{8}$$

To predict limiting cases, we write 1 in RHS as $(2/\pi)\int_0^\infty \sin(\lambda z)/\lambda\, d\lambda$. Then, for $R \to \infty$ or $\epsilon_a \ll \epsilon_s$ or $S \to R$, Eq. (8) reduces to the Inverse Fourier Sine Transform of the bulk expression for screening, $\varphi/V = \exp(-z/L_D)$. This is in conformity with the facts that the ambient field plays no role for $R \to \infty$ or $\epsilon_a \ll \epsilon_s$ and the system of closely packed nanowires ($S \to R$) resembles a bulk semiconductor. To complete the solution, we obtain φ as a function of r and z, by integrating the linear E_r versus r relation obtained from Eq. (5), as

$$\varphi(r,z) = \varphi(R^+,z) - \frac{R^2 - r^2}{2R}\frac{\epsilon_a}{\epsilon_s}\int_0^\infty A(\lambda)\lambda T(\lambda)\sin(\lambda z)\, d\lambda. \tag{9}$$

Fig. 3 presents φ versus z estimated from Eq. (8) and prior works.[4,5] Our results for arrays approach the bulk behavior as R is increased and the single NW behavior as S is increased. Our results for single NWs are within 2% of those of Ref. 5, which, however, does not treat arrays. On the other hand, Ref. 4, which treats arrays, does not capture ϵ_s dependence. Further, for realistic array geometries considered in Fig. 3, in Ref. 4, the potential in a NW of an array is higher and varies more gradually than that in a single NW, and deviates from the bulk potential as R is increased. For $R \ll S$ and $R \ll L_D$ considered in Ref. 4, results of Ref. 4 are inaccurate by 20%. These trends are due to the neglect of Poisson's equation in the NW, and assuming the NW to be a line charge for setting the boundary condition on E_r at $r = R$.

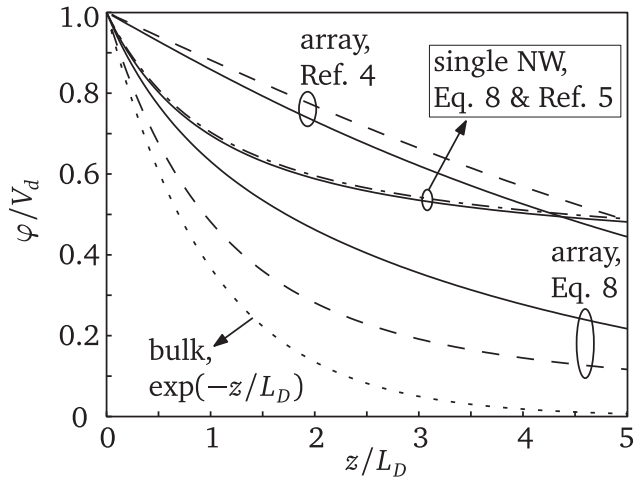

FIG. 3. The interface potential along wire length for small V_d. For the NW array: $S/R = 6$, and $R/L_D = 0.5$ (solid line) or 1.5 (dashed line). For the single NW: $R/L_D = 0.5$, dashed-dotted line is Ref. 5, and solid line is present work. $\epsilon_s/\epsilon_a = 3$.

We now consider the case of large V_d, where depletion is complete, and derive an expression for the depletion width W in a NW/NT Schottky junction. In a single long NW/NT, the screening is weak, and so, the tail of the junction space-charge region beyond the completely depleted portion extends over the entire length.[3] However, if the NW/NT is part of an array, this tail is short as in bulk, due to mutual screening from surrounding NWs/NTs.[5] The three boundary conditions at $r = 0$, $r = S$, and $z = 0$ are same as in the case of small V_d (see Fig. 2). The condition of $\varphi \to 0$ as $z \to \infty$ does not yield an analytical solution, and hence, the following alternative is employed. As in the 1D p-n junction analysis, we use the complete depletion approximation, i.e., for $0 < z \le W$, $\rho(r,z) = -qN_A$, and for $z > W$, $\rho(r,z) = 0$. Because of the absence of any charge beyond $z > W$, no field line crosses the plane $z = W$, and we set the boundary condition on $z = W$ to be $\partial\varphi/\partial z = 0$. Note that, $\varphi = V_d$ at $z = 0$ implies $\varphi = 0$ inside the NW at $z = W$. However, the plane $z = W$ cannot be assumed to be equipotential because the radial field terminating on the NW causes the potential to vary with r in the plane $z = W$.

Carrying out a derivation similar to Eqs. (1)–(8) for small V_d, we obtain φ for large V_d as

$$\varphi(r > R, z) = V_d - \sum_{m=0}^{\infty} B_m \sin(k_m z) \times \left\{ \frac{I_1(k_m S)K_0(k_m r) + I_0(k_m r)K_1(k_m S)}{I_1(k_m S)K_0(k_m R) + I_0(k_m R)K_1(k_m S)} \right\}, \tag{10}$$

where $k_m = (2m+1)\pi/2W$ and

$$B_m = \frac{16V_t(W/L_D)^2}{(2m+1)^3\pi^3\left[1 + 2\frac{\epsilon_a}{\epsilon_s}\frac{T(k_m)}{k_m R}\right]}. \tag{11}$$

Using the condition $\varphi(R^+, W) = 0$, from the above discussion in Eq. (10), we get $V_d = \sum_0^\infty (-1)^m B_m$. Here, we substitute for B_m from Eq. (11), and rearrange to obtain the following implicit equation for W, to be solved iteratively:

$$\frac{W}{W_B} = \sqrt{\alpha}\left[\sum_{m=0}^{\infty} \frac{(-1)^m/(2m+1)^3}{1 + \frac{2\epsilon_a}{\epsilon_s}\frac{T(k_m)}{k_m R}}\right]^{-\frac{1}{2}}, \tag{12}$$

where $W_B = \sqrt{2\epsilon_s V_d/qN_A}$ is the bulk depletion width and $\alpha = \sum_0^\infty (-1)^m/(2m+1)^3 \approx 0.97$. Equation (12) yields $W = W_B$ for $R \to \infty$ or $\epsilon_a \ll \epsilon_s$ or $S \to R$. For $W \gg R$, $T(k_m)/k_m R \to [(S/R)^2 - 1]/2$, and Eq. (12) gives

$$W \approx W_B\sqrt{1 + \frac{\epsilon_a}{\epsilon_s}\left[\left(\frac{S}{R}\right)^2 - 1\right]} \text{ for } W \gg R. \tag{13}$$

This yields the important result: W in a NW array is approximately S/R times W_B and varies as $1/R\sqrt{qN_A}$. We conclude from Eq. (13) that W in a NW array can be much larger than W_B depending on the inter-wire separation, and that the dependence of W on doping and potential drop is still square root, as in a planar bulk junction. This is in contrast with the exponential form of earlier expression $W = R\exp(4\epsilon_a V_d/qN_A R^2)$ derived for both a single NW[5,6] and a NW in an array[4] having $S \gg W \gg R$. Further, the earlier expression[4–6] does not capture ϵ_s dependence. Exact W for any geometry (set $S \to \infty$ in case of single NW) can be obtained from Eq. (12), which is valid without restriction. This W matches with the W (see Fig. 4) extracted from self-consistent numerical calculations of Poisson's equation and drift-diffusion current density equations,[13] as the point at which the space charge density falls to 42.4% of the maximum. This criterion is analogous to that in a bulk Schottky junction, where the numerically calculated charge density falls to 42.4% of the maximum at the depletion edge $W_B = \sqrt{2\epsilon_s V_d/qN_A}$ derived from the 1D p-n junction analysis (See Fig. 5). The inset of Fig. 4 reveals that W of a NW approaches W_B for $R/W_B > 0.5$ irrespective of the value of S/R.

We now derive the depletion width for an array of NTs, considering n-type doping without loss of generality. From an electrostatic viewpoint, a NT array is analogous to a NW array with $\epsilon_s = \epsilon_a$ and zero space-charge but non-zero

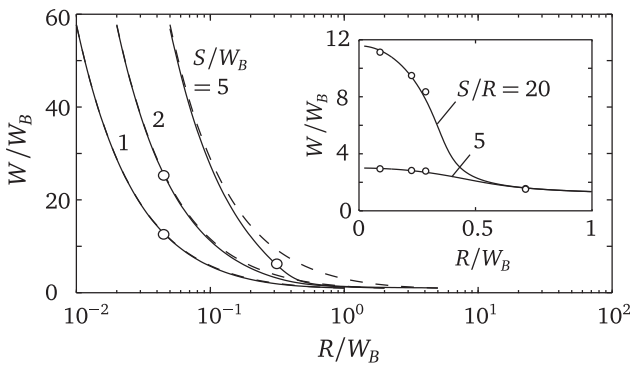

FIG. 4. Depletion width of a NW array versus NW radius for $\epsilon_s/\epsilon_a = 3$ and different values of S and S/R (inset). Legend: solid lines–Eq. (12), dashed lines–Eq. (13), circles–simulations (Si NW in SiO_2 ambient, $N_A = 10^{16}, 10^{17}\,\text{cm}^{-3}$, $V_d = 0.4\,\text{V}$, $R = 10, 20, 50, 70\,\text{nm}$).

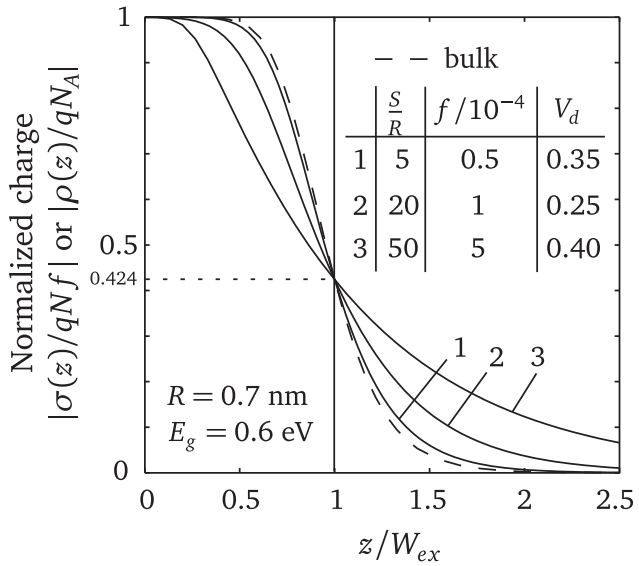

FIG. 5. Normalized surface charge $(\sigma(z)/qNf)$ versus z/W$_{ex}$, where W_{ex} is the extracted depletion width of the respective NT structure from numerical calculations. $\epsilon_a = 3.9\epsilon_0$.

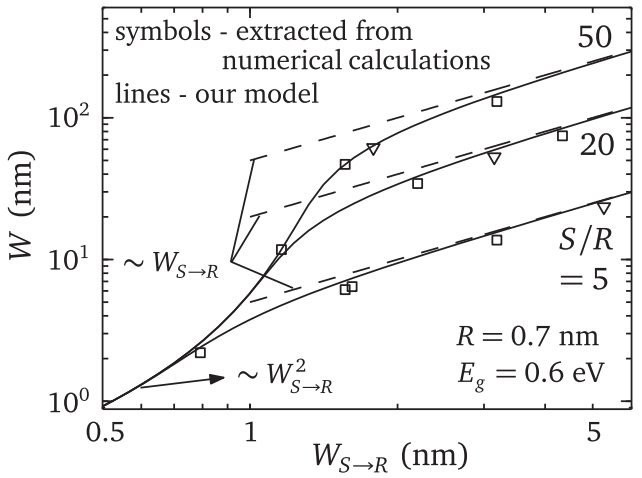

FIG. 6. Showing the dependence of the depletion width of a NT array on V_d, f, R, and S in a single plot; $W_{S\to R} = \sqrt{\epsilon_a V_d R/qNf}$. Legend: solid lines–Eq. (12) modified for a NT array, dashed lines–Eq. (14). The triangle symbols correspond to NT structures of Fig. 5; for the square symbols, following values are employed: $f = 5\times10^{-5}$, 1×10^{-4}, 5×10^{-4}, 1×10^{-3}; $\epsilon_a = \epsilon_0$, $3.9\epsilon_0$; V_d is set equal to $(E_F - E_i)/q$.

interface charge $\sigma_0 = qNf$, N = areal density of carbon atoms, f = doping fraction. Hence, we obtain the model for a NT array by using Eq. (1) with $\rho = 0$, Eq. (2) modified as per $-\partial\varphi(R^+,z)/\partial r + \partial\varphi(R^-,z)/\partial r = \sigma_0/\epsilon_a$, Eq. (3) as it is, and following through the NW procedure thereafter. The model for W of a NT array is same as Eq. (12) with ϵ_s replaced by ϵ_a and W_B by $W_{S\to R} = \sqrt{\epsilon_a V_d R/qNf}$. This W reduces to

$$W \approx (S/R)W_{S\to R} \quad \text{for large} \quad W_{S\to R}\,, \tag{14}$$

where large $W_{S\to R}$ translates to $W \gg R$. Equation (14) yields the important result $W \sim 1/\sqrt{Rf}$. This can be unified with the behavior $W \sim 1/R\sqrt{qN_A}$ derived above for a NW array as $W \sim 1/\sqrt{\text{charge per unit length}}$, where the charge per unit length $= \pi R^2 qN_A$ for a NW and $= 2\pi RqNf$ for a NT. Further, $W \propto S$ from Eqs. (13) and (14). These results are valid for $W \gg R$, which usually holds for a wide range of NW/NT structures.

We validate our model by comparing it with numerical calculations of a Carbon Nanotube (CNT) array. We write the CNT charge as[3]

$$\sigma(z) = qNf - qN\int_{E_c(z)}^{\infty} D(E,z)F(E)\,dE\,, \tag{15}$$

where

$$D(E,z) = \frac{a\sqrt{3}}{\pi^2 RV_0}\sum_{m=-\infty}^{m=\infty} g[E - E_c(z) + Eg/2, \varepsilon_m] \tag{16}$$

is the universal density of states function,[14] modified as per local $E_c(z)$, and $F(E)$ is the Fermi function. $g(E,\varepsilon) = |E|/\sqrt{E^2-\varepsilon^2}$ for $|E| > \varepsilon$ and zero otherwise, and $\varepsilon_m = |3m+1|aV_0/2R$. $V_0 = 2.5$ eV is the π-band tight-binding parameter, and a is the C-C bond length. Using Finite Difference Method, we self-consistently solve Eq. (15), the Laplace's equation $\nabla^2\varphi = 0$ both inside and outside the NT, and $-\partial\varphi(R^+,z)/\partial r + \partial\varphi(R^-,z)/\partial r = \sigma(z)/\epsilon_a$. We consider L to be greater than W so that the charge tail goes to zero at $z = L$, and set the boundary condition at $z = L$ as $\partial\varphi/\partial z = 0$.

In Fig. 5, we plot the numerical calculations of $\sigma(z)$ versus z in a normalized form to compare it with the bulk behavior. As mentioned earlier in case of NW, we locate the depletion width at the point where the charge density falls to 42.4% of σ_0. We notice from Fig. 5 that the NT behavior is similar to bulk behavior, except that the rate at which the charge density tails off depends on S, f, and ϵ_a. In Fig. 6, we plot W of a NT array as a function of $W_{S\to R}$. We see our model matches well with the numerical calculations. Further, W varies as $\sim W_{S\to R}^2 \sim V_d/f$ for small $W_{S\to R}$ (i.e., small V_d or large f), and as $\sim W_{S\to R} \sim \sqrt{V_d/f}$ for large $W_{S\to R}$ (i.e., large V_d or small f). This is in contrast with the exponential form predicted in Ref. 3 for a single NT.

Note that V_d is the potential drop in the NW/NT, so $V_d = V_{bi} - V_a$, where V_{bi} is the built-in potential and V_a is the applied voltage. It is shown in Ref. 15 that Fermi-level pinning has no effect on the barrier height of a Schottky NT junction, implying $V_{bi} = \varphi_{ms}$, where φ_{ms} is the work-function difference. This is because, the charge due to interface states forms a tiny dipole ring (a tiny dipole disc in case of NW), whose electrostatics differs from that of the large dipole sheet in a planar bulk junction. If the NW is very thin, the density of states function would be different from that of bulk. While this affects φ_{ms} and hence V_d, it does not affect our model that relates W to V_d and N_A. If the NW/NT is short, entire wire/tube will be completely depleted,[9] in which case V_d can be obtained from $V_d = \sum_0^\infty (-1)^m B_m$ by substituting the wire/tube length for W in B_m.

In conclusion, we developed a simple, accurate, and unified analytical model of the junction electrostatics of NW/NT arrays, extendible to nanofilms. The model predicts accurately the large depletion width, and gives following simple results for NW/NT arrays wherein the depletion width is much greater than the NW/NT radius. First, the depletion width dependence on doping and potential drop is square

root, like in a bulk junction and unlike the exponential dependence derived in literature for a single NW/NT. Second, the depletion width varies as $1/\sqrt{\text{charge per unit length}}$ multiplied by inter-wire/tube separation, where charge per unit length includes the effects of wire/tube radius and doping. The model should be useful in the design of nanoscale Schottky diodes, photodiodes, solar cells, etc.

[1]J. Goldberger, A. I. Hochbaum, R. Fan, and P. Yang, Nano Lett. **6**, 973 (2006).
[2]A. D. Franklin and Z. Chen, Nat. Nanotechnol. **5**, 858 (2010).
[3]F. Léonard and J. Tersoff, Phys. Rev. Lett. **83**, 5174 (1999).
[4]H. Ruda and A. Shik, Appl. Phys. Lett. **85**, 1030 (2004).
[5]A. Achoyan, S. Petrosyan, W. Craig, H. Ruda, and A. Shik, J. Appl. Phys. **101**, 104308 (2007).
[6]F. Léonard, A. A. Talin, B. Swartzentruber, and S. Picraux, Phys. Rev. Lett. **102**, 106805 (2009).
[7]J. Hu, Y. Liu, A. Maslov, C.-Z. Ning, R. Dutton, and S.-M. Kang, Proc. SPIE **6468**, 64681E (2007).
[8]J. Hu, Y. Liu, C.-Z. Ning, R. Dutton, and S.-M. Kang, Appl. Phys. Lett. **92**, 083503 (2008).
[9]M. Zervos, Semicond. Sci. Technol. **23**, 075016 (2008).
[10]K. Maheswaran and S. Karmalkar, Physica E **44**, 700 (2011).
[11]N. Averkiev and A. Shik, Phys. Rev. B **59**, 3250 (1999).
[12]X.-G. Zhang and S. T. Pantelides, Nano Lett. **9**, 4306 (2009).
[13]*Sentaurus Device User Guide*, Synopsys, 2013.
[14]J. Mintmire and C. White, Phys. Rev. Lett. **81**, 2506 (1998).
[15]F. Léonard and J. Tersoff, Phys. Rev. Lett. **84**, 4693 (2000).